Phonon-packet propagation through solid-liquid interfaces: resonant effects in the presence of a superlattice

2000 J. Phys.: Condens. Matter 12 9843

(http://iopscience.iop.org/0953-8984/12/48/303)

J. Phys.: Condens. Matter **12** (2000) 9843–9855. Printed in the UK PII: S0953-8984(00)13017-6

Phonon-packet propagation through solid–liquid interfaces: resonant effects in the presence of a superlattice

K Imamura, Y Tanaka, S Mizuno and S Tamura
Department of Applied Physics, Hokkaido University, Sapporo 060-8628, Japan

Received 3 April 2000, in final form 4 August 2000

Abstract. Phonon transmission through a solid–liquid interface is enhanced resonantly when a periodic, elastic multilayer (a superlattice) is inserted at the interface. This happens either at an eigenfrequency ($\tilde{\nu}$) of the vibrational mode localized at a superlattice–liquid interface or at a frequency (ν_0) of the extended vibrational state characteristic of a structure with coupled bilayers. We study the unusual features associated with these resonances by considering the transmission and reflection of rectangular phonon packets (with a peak at a $\tilde{\nu}$ or at ν_0 in the frequency space) by numerical simulations. A significant aspect predicted is the universal double-peak structure of the reflected packet, which we can reproduce well by analytic calculations. Numerical examples are developed for systems consisting of a nanometre-scale GaAs/AlAs superlattice inserted at a GaAs–H_2O interface and a millimetre-scale Al/polymer multilayer inserted at an Al–H_2O interface.

1. Introduction

The rate of transmission of phonons or sound waves through a single solid–liquid interface is small in general due to the large acoustic mismatch between solid and liquid [1]. For instance, for the normal incidence of longitudinal phonons the energy transmission rate is about 0.2 at a GaAs/H_2O interface. Recently, Kato [2] has shown by numerical calculation with a transfer-matrix method that the transmission rate of phonons at a solid–liquid interface is enhanced sharply (up to $\simeq 1$) at certain isolated frequencies ($\tilde{\nu}$) when a periodic, elastic multilayer (a superlattice) is inserted at the interface. These frequencies $\tilde{\nu}$ coincide within the numerical error with the eigenfrequencies of the vibrational mode localized at the free surface of the superlattice inserted [3, 4]. Thus we understand that the enhanced transmission is caused by the resonant interaction between the incident phonon and a localized vibration which still exists in the superlattice near the surface in contact with liquid. This 'localized' vibration is, however, extended on the liquid side, so is more precisely semi-localized—but we call it 'localized' rather than semi-localized, for brevity [5].

An interesting feature not recognized by Kato is the fact that the magnitude of the transmission peak at $\tilde{\nu}$ is sensitive to the number of bilayers N of the superlattice. Recently one of the present authors derived analytically the equation for determining the value $N = N_{max}$ for which the transmission rate takes a maximum value for a given combination of the solid, superlattice and liquid [6].

Experimentally, phonons or ultrasound are usually excited and launched in the form of a pulse or a packet rather than the monochromatic plane wave studied theoretically. Hence, for the experimental verification of the predicted anomalous transmission it is important to analyse the expected behaviour of phonon packets or phonon pulses which are composed of

0953-8984/00/489843+13$30.00

phonons in a finite range of frequencies (including a resonant frequency) rather than that of a single-frequency phonon. These entities are also localized in space and time and hence suitable for use in studying the time-dependent aspects of the resonance associated with the phonon propagating through the solid–superlattice–liquid structure. (For example, the width or lifetime of the resonance is measured by the slopes of the tails of the transmitted and reflected packets.) Such temporal behaviour of phonon packets is also related to the phases of the transmission and reflection coefficients [4, 7], which were not studied by Kato and in reference [6].

The purpose of the present paper is thus to study the unusual aspects associated with the transmission and reflection of phonon packets propagating from solid to liquid and vice versa in the presence of a periodic superlattice inserted at the solid–liquid interface. In particular, we consider the cases where the incident packets have rectangular shapes. The reasons are as follows:

(1) The rectangular packets define their wave fronts sharply and hence are suitable for use in discussing the time delay and/or advance of the transmitted and reflected packets.
(2) They make it rather easy to identify which part of the incident packet is effectively transmitted or reflected by the interaction with the superlattice. For Gaussian packets which were used previously in the simulations of phonon transmission through superlattices [4, 7] it is rather hard to define their front and rear edges and hence they make the discussion of the associated delay and/or advance ambiguous.
(3) More importantly, the rectangular packets have been generated as tone-burst excitations of ultrasound in a MHz frequency range. They have recently been applied to the experimental study of the transmission characteristics of low-frequency phonons in one-dimensional (1D) and 2D periodic multilayers [8, 9].

For numerical examples we consider two cases where the solid multilayers inserted are a conventional semiconducting superlattice of nanometre dimensions and a macroscopic superlattice of millimetre dimensions. In the former case the resonance frequencies are several hundred GHz which can be probed, for example, by picosecond-light-pulse methods [1, 3]. In the latter case they should be found in a MHz frequency range, accessible to ultrasound transmission experiments [8].

In the next section we formulate the characteristics of transmission of phonons between a solid and a liquid in the presence of periodic multilayers at the interface. Specifically, the condition is given for the number of bilayers N_{max} at which the transmission rate takes a maximum value in a solid–superlattice–liquid structure. In section 3 we derive for a rectangular incident packet the analytic expressions for the asymptotic shapes of the transmitted and reflected wave packets. Numerical simulations are developed in section 4 for the transmission and reflection of phonon packets in a GaAs–$(GaAs/AlAs)_N$–H_2O system and ultrasound packets in an Al–$(Al/polymer)_N$–H_2O system, where the initial packets propagate from the liquid side. We also explain the physical origins of the predicted features associated with the packet propagations. Concluding remarks are given in section 5.

2. Transmission characteristics of phonons

Here we summarize the transmission characteristics of the longitudinal phonons incident normally to the solid (S)–superlattice–liquid (L) interface. In this system the phonon transmission rate T is calculated analytically on the basis of the transfer-matrix method which has been used repeatedly in the literature [4, 7, 10]. The result for the propagation from the solid

to the liquid side is [10]

$$T = \left(4\frac{Z_L}{Z_S}\right) \Big/ \left[\left(\frac{Z_L}{Z_A}T_{12} - \frac{Z_A}{Z_S}T_{21}\right)^2 + \left(T_{22} + \frac{Z_S}{Z_L}T_{11}\right)^2\right] \tag{1}$$

where the superlattice is assumed to consist of A and B layers with the A layer adjacent to the solid and the B layer adjacent to the liquid as shown in the inset of figure 1. In equation (1) Z is the acoustic impedance defined by the product of the mass density ρ and the sound velocity v as $Z = \rho v$ and T_{ij} is a matrix element of the 2×2 transfer matrix for the periodic superlattice, for which explicit expressions are given in reference [10]. An important observation is the fact that the transmission rate equation (1) is the same for the phonon propagation from the solid side to the liquid side as vice versa. This 'reciprocity relation' for the phonon transmission rate can be seen from the fact that equation (1) is symmetric under the interchanges S $\leftrightarrow$ L and A $\leftrightarrow$ B together with $T_{11} \leftrightarrow T_{22}$, $T_{12} \rightarrow -T_{12}$ and $T_{21} \rightarrow -T_{21}$ [10].

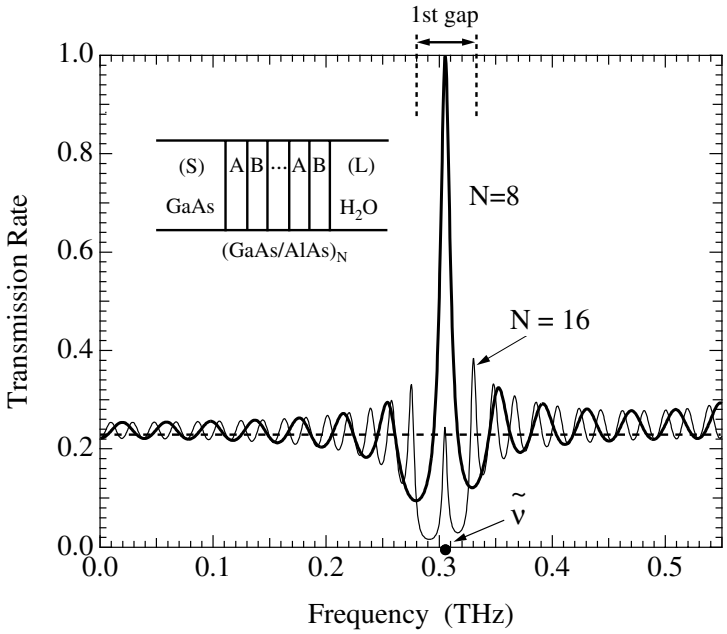

Figure 1. The frequency dependence of the phonon transmission rate (longitudinal mode) in the GaAs–$(GaAs/AlAs)_N$–H_2O system shown in the inset with $N = 8$ (bold line) and $N = 16$ (thin solid line). The unit period of the superlattice consists of GaAs and AlAs layers each consisting of fifteen monolayers. The horizontal dashed line marks the rate of transmission through a single GaAs–H_2O interface. (These results are valid for phonons propagating from GaAs to the H_2O side and vice versa.) The narrow frequency region in between the two vertical dashed lines is the lowest frequency gap of the superlattice and $\tilde{\nu} = 305$ GHz is the eigenfrequency of the surface localized vibration within this gap.

To avoid unnecessary complication, we hereafter assume that $Z_S = Z_A$. Then we consider equation (1) under the condition that the localized vibration exists at the free surface of the superlattice (with the B surface layer) when the liquid is removed. This condition is equivalent to $Z_B < Z_A$ [3, 4]. In this case the eigenfrequency of the surface localized mode $\tilde{\omega} \equiv 2\pi\tilde{\nu}$ appears inside the frequency gap of the perfect, periodic superlattice and its expression is

$$\tilde{\omega} = \omega_m + \frac{\varepsilon}{2\pi}\omega_1 \sin\left(\frac{2\omega_m d_A}{v_A}\right) \tag{2}$$

where, $\omega_m = m\omega_1 = m\pi(d_A/v_A + d_B/v_B)^{-1}$ ($m = 1, 2, 3, \ldots$) is the mth-order Bragg frequency and $\varepsilon = Z_B/Z_A - 1 < 0$. For the majority of superlattices, Z_A is close to Z_B, i.e., $|\varepsilon| \ll 1$, and the second term of equation (2) can be neglected.

At a frequency ω close to $\tilde{\omega} \simeq \omega_m$ we have the resonant form for the transmission rate:

$$T = \frac{4\delta}{C(\omega - \tilde{\omega})^2 + (\delta e^{-N\varepsilon} + e^{N\varepsilon})^2} \tag{3}$$

where

$$C = (1+\delta)^2 \frac{\pi^2}{\omega_1^2} \frac{\sinh^2 N\varepsilon}{\varepsilon^2}. \tag{4}$$

N is the number of bilayers and $\delta = Z_L/Z_S$. The transmission from the solid to the liquid and vice versa through the superlattice is found to be complete, or $T(\tilde{\omega}) = 1$, when

$$\delta = e^{2N\varepsilon}. \tag{5}$$

Because N is an integer, the transmission rate has a maximum value for the periodicity number N_{max} closest to

$$N = \frac{1}{2|\varepsilon|} \ln \frac{Z_S}{Z_L}. \tag{6}$$

If equation (5) or equivalently equation (6) is satisfied, the transmission rate takes the Breit–Wigner form:

$$T = \frac{\gamma^2}{(\omega - \tilde{\omega})^2 + \gamma^2} \tag{7}$$

where the width γ is given by

$$\gamma = \frac{4\varepsilon\omega_1}{\pi}(\delta^{-1} - \delta)^{-1} = \frac{4\varepsilon\omega_1}{\pi}\left(\frac{Z_A}{Z_L} - \frac{Z_L}{Z_A}\right)^{-1}. \tag{8}$$

Equation (8) is valid for $Z_S = Z_A$. For a more general case with $Z_S \neq Z_A$, equation (8) should be replaced by [6]

$$\gamma = \frac{4\varepsilon\omega_1}{\pi}\left(\frac{Z_S}{Z_A} - \frac{Z_A}{Z_S} + \frac{Z_A}{Z_L} - \frac{Z_L}{Z_A}\right)^{-1}. \tag{9}$$

Figure 1 illustrates the frequency dependence of the transmission rate T in the GaAs–(GaAs/AlAs)$_N$–H_2O system†, where the unit period of the superlattice consists of GaAs and AlAs layers each consisting of fifteen monolayers. We see a large enhancement in transmission at $\nu = \tilde{\nu} = 305$ GHz when the superlattice of eight periods ($N = 8$) is sandwiched in between bulk GaAs and water. This enhanced transmission occurs only when the layer adjacent to the water is AlAs (B layer) with acoustic impedance ($Z_{AlAs} = Z_B = 2.12 \times 10^6$ g cm^{-2} s^{-1}) smaller than that of GaAs ($Z_{GaAs} = Z_A = 2.52 \times 10^6$ g cm^{-2} s^{-1}). The peak frequency $\tilde{\nu}$ is situated inside the lowest frequency gap of the phonons in the superlattice. For comparison, the corresponding result for $N = 16$ is also shown in figure 1. For this number of periods a transmission peak is again found at almost the same frequency but its magnitude is small and similar to the value at the single GaAs–H_2O interface ($T \simeq 0.2$) plotted as the dashed line.

Figure 2 shows how the magnitude of the transmission peak at $\nu = \tilde{\nu}$ changes with the periodicity number N of the superlattice. The highest transmission rate is attained at $N = N_{max} = 8$ for water ($Z_L = Z_{H_2O} = 1.48 \times 10^5$ g cm^{-2} s^{-1}) in contact with the GaAs/AlAs superlattice but it occurs at $N_{max} = 20$ if the water is replaced with liquid helium ($Z_L = Z_{^4He} = 2.99 \times 10^3$ g cm^{-2} s^{-1}) with much smaller acoustic impedance.

† The numerical values of the longitudinal sound velocity used are $v_{GaAs} = 4.71 \times 10^5$ cm s^{-1} and $v_{AlAs} = 5.65 \times 10^5$ cm s^{-1} for GaAs and AlAs, respectively, and the mass densities are $\rho_{GaAs} = 5.36$ g cm^{-3} for GaAs and $\rho_{AlAs} = 3.76$ g cm^{-3} for AlAs.

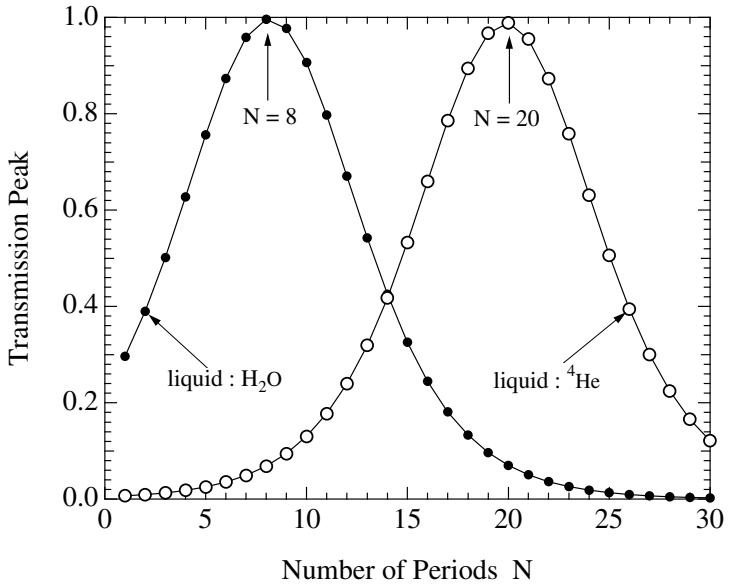

Figure 2. The magnitude of the transmission peak versus the number of periods N of the GaAs–(GaAs/AlAs)$_N$–liquid system at $\nu = \tilde{\nu} = 305$ GHz. The liquids considered are H_2O (filled circles) and ^{4}He (open circles).

Briefly, the physical reason for the existence of a finite N_{max} is understood as follows. First we note that the enhanced transmission is caused by the resonance of an incident phonon with the vibration localized in the superlattice near the liquid interface. Thus the lattice displacement associated with this vibration increases exponentially in the superlattice from the solid side to the liquid side. (At $\nu = \tilde{\nu}$ the lattice displacements u between adjacent nth and $(n+1)$th periods in the superlattice are expressed as $u_{n+1}/u_n \simeq \mathrm{e}^{|\varepsilon|}$.) Such an increasing amplitude towards the liquid side (or equivalently decreasing amplitude towards the solid side) is allowed because the acoustic energy flux is given by $P_\mathrm{I} \sim \omega^2 Z_\mathrm{I}|a_\mathrm{I}|^2$ (I = S, L and a_I is the displacement amplitude) and Z_L is much smaller than Z_S. Hence, the amplitude $|a_\mathrm{L}|$ in liquid can be much larger than $|a_\mathrm{S}|$ in solid, but of course not indefinitely. As the number of bilayers N increases, the growth (due to the resonance) of the displacement amplitude at the superlattice–liquid interface will eventually violate the acoustic energy conservation for the solid and liquid. Thus there should exist a maximum number N_{max} and for $N > N_{max}$ the decreasing amplitude towards the liquid side becomes dominant and accordingly the transmission rate decreases.

The maximum periodicity number of the superlattice N_{max} is the one for which the transmitted energy flux may be equal to or slightly less than the incident energy flux of phonons. The reciprocity relation of the transmission rate ensures that the anomalous transmission is realized at the same value N_{max} for the phonon propagations from the solid to the liquid side and the liquid to the solid side.

3. Expressions for the transmitted and reflected phonon packets

Here we derive approximate expressions for the shapes of the transmitted and reflected phonon packets propagating in the system studied. First we write the incident packet Ψ_i

as a superposition of plane waves:

$$\Psi_i(z,t) = \int \mathrm{d}\omega\, \phi(\omega) \exp[\mathrm{i}(kz - \omega t)] \tag{10}$$

where the z-direction is normal to the interface between the solid and the liquid, $k = \omega/v_\mathrm{I}$ is the wavenumber and the coefficient ϕ is given by $\phi(\omega) = \phi_0 \sin(\omega a/v_\mathrm{I})/\pi\omega$ (with ϕ_0 an amplitude) for a packet of rectangular shape of width $2a$. Also I = S or L depending on the region in which the incident packet propagates. Similarly, the transmitted and reflected packets Ψ_t and Ψ_r in the asymptotic regions take the forms

$$\begin{pmatrix} \Psi_t \\ \Psi_r \end{pmatrix} = \int \mathrm{d}\omega\, \phi(\omega) \begin{pmatrix} t(\omega) \\ r(\omega) \end{pmatrix} \exp[\mathrm{i}(\pm kz - \omega t)] \tag{11}$$

where t and r are the amplitude transmission and reflection coefficients, respectively. Near $\omega = \tilde{\omega}$ the transmission and reflection coefficients are well approximated by the following forms characteristic of the resonance [7]:

$$\begin{aligned} t(\omega) &= \frac{\mathrm{i}\alpha\gamma}{\omega - \tilde{\omega} - \mathrm{i}\gamma} \mathrm{e}^{-\mathrm{i}kD} \\ r(\omega) &= \frac{\beta(\omega - \tilde{\omega})}{\omega - \tilde{\omega} - \mathrm{i}\gamma} \end{aligned} \tag{12}$$

where D is the thickness of the superlattice and α and β are constants which contain neither k nor ω, and their explicit expressions are not required in the present calculation. We also note that equation (8) can be used for γ for the propagation of phonons from the solid to the liquid side, but for the propagation from the liquid to the solid side we have to use a somewhat complicated expression for γ (derived with the use of equation (9)):

$$\gamma = \frac{4\,\omega_\mathrm{I}}{\pi} |\tilde{\varepsilon}| \left(\frac{Z_\mathrm{L}}{Z_\mathrm{B}} - \frac{Z_\mathrm{B}}{Z_\mathrm{L}} + \frac{Z_\mathrm{B}}{Z_\mathrm{A}} - \frac{Z_\mathrm{A}}{Z_\mathrm{B}} \right)^{-1} \tag{13}$$

where $\tilde{\varepsilon} = Z_\mathrm{A}/Z_\mathrm{B} - 1 = -(Z_\mathrm{A}/Z_\mathrm{B})\varepsilon$ [6]. In these equations the solid is still assumed to be the same as the A material, or $Z_\mathrm{S} = Z_\mathrm{A}$.

We apply these expressions to the case where the initial phonon packet propagates from the liquid side to the solid side through the superlattice. This configuration is more suitable for the ultrasound transmission experiment with immersion transducers, but qualitatively the same results are obtained for the other configuration because of the reciprocity relation of the transmission rate.

The integration of equation (11) with equation (12) now leads to

$$\begin{aligned} \Psi_t = \frac{1}{2} A_0 \exp(\mathrm{i}\tilde{K}_\mathrm{S} x_\mathrm{S}) \{ &\theta(x_\mathrm{S} - \tilde{a}) - \theta(x_\mathrm{S} + \tilde{a}) \\ &+ \theta(-x_\mathrm{S} - \tilde{a})[1 - 2\mathrm{e}^{\Gamma_\mathrm{S}(x_\mathrm{S} + \tilde{a})}] - \theta(-x_\mathrm{S} + \tilde{a})[1 - 2\mathrm{e}^{\Gamma_\mathrm{S}(x_\mathrm{S} - \tilde{a})}] \} \end{aligned} \tag{14}$$

$$\Psi_r = B_0 \exp(-\mathrm{i}\tilde{K}_\mathrm{L} x_\mathrm{L}) [\theta(x_\mathrm{L} + a)\mathrm{e}^{-\Gamma_\mathrm{L}(x_\mathrm{L} + a)} - \theta(x_\mathrm{L} - a)\mathrm{e}^{-\Gamma_\mathrm{L}(x_\mathrm{L} - a)}] \tag{15}$$

where $A_0 = \alpha\phi_0$, $B_0 = \beta\phi_0$, $\tilde{a} = (v_\mathrm{S}/v_\mathrm{L})a$, $\tilde{K}_\mathrm{I} = \tilde{\omega}/v_\mathrm{I}$, $\Gamma_\mathrm{I} = \gamma/v_\mathrm{I}$ (I = S, L), $x_\mathrm{S} = z - v_\mathrm{S}t - D$, $x_\mathrm{L} = z + v_\mathrm{L}t$ and $\theta(x)$ is a unit-step function, i.e., $\theta(x) = 1$ for $x \geqslant 0$ and $\theta(x) = 0$ for $x < 0$. The amplitudes $|\Psi_t|$ and $|\Psi_r|$ given by equations (14) and (15) are illustrated in figure 3 for $\gamma a/v_\mathrm{L} = 10$ and $v_\mathrm{S} = 2v_\mathrm{L}$. Comparing with the shape of the incident packet, the front part of the transmitted packet is reduced and it is followed by a tail exponentially decaying at the rate determined by the width γ of the resonance. A more prominent feature is the double-peak structure of the reflected packet. These double peaks are identical to each other and are again associated with the decaying tails determined by γ.

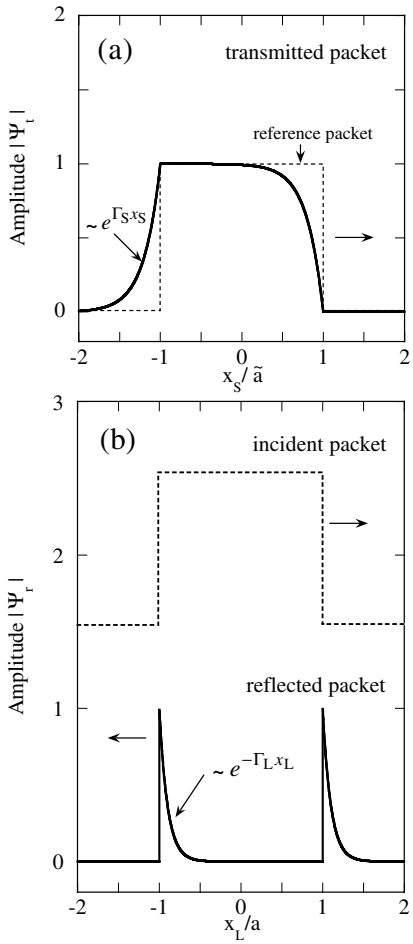

Figure 3. Analytically calculated asymptotic shapes of (a) transmitted ($\tilde{a} = (v_S/v_L)a$) and (b) reflected phonon packets (equations (14) and (15)) for the rectangular initial packet shown by the dashed line in (b). The dashed line in (a) is the reference packet which should appear in the solid if the transmission through the interface is perfect. The parameters taken for this figure are $\gamma a/v_L = 10$, $v_S = 2v_L$ and $A_0 = B_0 = 1$. Arrows indicate the directions of propagation for these packets.

The occurrence of these characteristic shapes is interpreted physically as follows: as remarked repeatedly, the enhanced transmission of phonons happens as a result of the resonant interaction between the incident phonon and the localized vibration at $\omega = \tilde{\omega}$. The localized state has a width γ in the frequency space and hence it should take a finite time γ^{-1} to excite this vibration at the superlattice–liquid interface. Thus, within the time interval γ^{-1} after the incident packet hits the superlattice, the transmission via the resonant interaction should be incomplete and this produces the reflected component of the packet as the first peak. Once the localized vibration is built up, the transmission of the incident phonon assisted by the resonance becomes complete and no reflected phonon appears. After the incident packet passes through the superlattice, the excited localized state decays with its lifetime γ^{-1} by emitting phonons on either side of the superlattice. This produces the exponentially decaying tail of the transmitted packet and the second peak of the reflected packet.

4. Numerical results

For numerical calculations we consider:

(A) the GaAs–(GaAs/AlAs)$_N$–H_2O system where the superlattice is of nanometre dimensions consisting of 15-monolayer GaAs and 15-monolayer AlAs with the number of bilayers $N = 8$; and

(B) the Al–(Al/polymer)$_N$–H_2O system [9]† where the superlattice has a millimetre-scale thickness, consisting of 0.5 mm thick Al and 0.5 mm thick polymer (Crystalbond) with $N = 3$.

We also assume incident phonon packets of rectangular shapes whose peaks in the frequency space coincide with the peaks of the anomalous transmission. As we remarked in section 3, the configuration where the initial phonon packet propagates from the liquid side is more suitable than the other one for the currently executed ultrasound experiments with immersion transducers. So, for the sake of comparison we assume this propagation configuration for both the GaAs–(GaAs/AlAs)$_N$–H_2O and Al–(Al/polymer)$_N$–H_2O systems.

4.1. GaAs–(GaAs/AlAs)$_N$–H_2O

The rate of transmission of phonons in this system is shown in figure 4(b). Large enhancements ($T \simeq 1$) are found inside the first and third frequency gaps of the phonons in the periodic GaAs/AlAs superlattice [4]. (The reason for the absence of a peak in the second gap is given in reference [4].) The peak frequencies in transmission coincide with the eigenfrequencies of the vibrational modes in the superlattice localized at the superlattice–liquid interface (dots in figure 4(a)). Figure 4(c) also indicates that at these frequencies large phase times are assigned to the transmitted phonons. The phase time is defined as the derivative of the phase of the transmission (or reflection) coefficient with respect to frequency and it describes the delay (if positive) or advance (if negative) of phonons transmitted through (or reflected from) the superlattice [11–13]. Here we note that the time needed for a phonon to propagate through the (GaAs/AlAs)$_8$ multilayers without any interference effect is 13.2 ps and the time delay (about 22 ps from figure 4(c)) is about twice this value.

For the simulations we assume an initial packet whose distribution in the frequency space is well confined inside the resonance peak of transmission (as illustrated in the inset of figure 5(a)). Figure 5 exhibits snapshots of the transmitted and reflected phonon packets after they have become well separated from the GaAs–(GaAs/AlAs)$_N$ and (GaAs/AlAs)$_N$–H_2O interfaces. The initial packet is assumed to propagate from the liquid side and the upper and lower parts show the results without and with GaAs/AlAs multilayers (with $N = 8$), respectively. The reference packets shown are those expected to appear when they are perfectly transmitted through or reflected back from the interface. The distribution of the packet in GaAs is broader due to the fact that the longitudinal sound velocity $v_{GaAs} = 4.71 \times 10^5$ cm s^{-1} ($=v_S$) in GaAs is much faster than the velocity $v_{H_2O} = 1.48 \times 10^5$ cm s^{-1} ($=v_L$) in H_2O.

No prominent feature is seen for the transmission and reflection of the packet through a single GaAs–H_2O interface. However, in the presence of the GaAs/AlAs superlattice the results are quite different. As expected from the analytical results given in figure 3, the front part of the transmitted packet is reduced and at the same time the exponentially decreasing tail is added to the rear part. As a result, the centroid of the transmitted packet is shifted afterwards,

† The longitudinal sound velocities used are $v_{Al} = 6.37 \times 10^5$ cm s^{-1} for aluminium and $v_{CB} = 4.69 \times 10^5$ cm s^{-1} for the polymer (Crystalbond). The mass densities are $\rho_{Al} = 2.7$ g cm^{-3} for aluminium and $\rho_{CB} = 1.35$ g cm^{-3} for the polymer (Crystalbond).

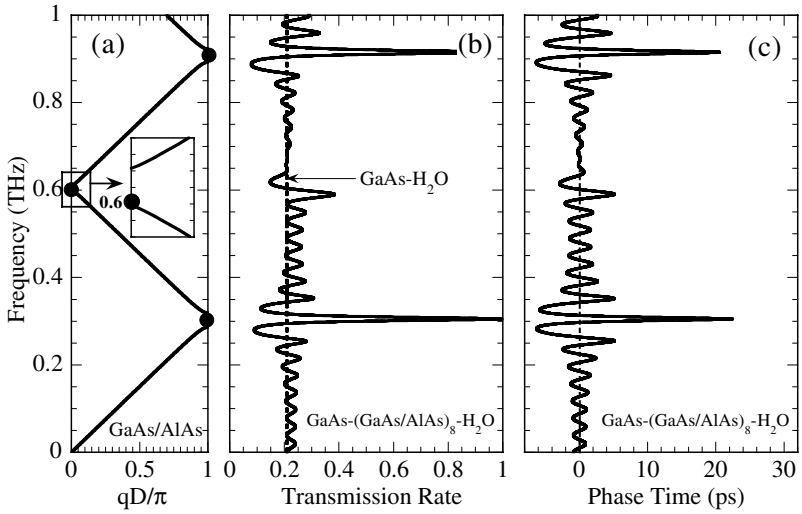

Figure 4. Comparison of (a) dispersion curves (longitudinal mode) in the perfect GaAs/AlAs superlattice, (b) the transmission rate and (c) the phase time of the transmitted phonons in the GaAs–$(GaAs/AlAs)_8$–H_2O structure. Dots in (a) indicate the eigenfrequencies of the surface localized vibration in the semi-infinite GaAs/AlAs superlattice and the dashed line in (b) indicates the rate of transmission through a single GaAs–H_2O interface. The parameters taken are the same as for figure 1.

leading to an appreciable time delay for the transmitted packet. Also, the reflected packet exhibits a double-peak structure similar to the one obtained by the analytical calculation. The finite amplitude in between the two peaks arises from the fact that the transmission coefficient is not well approximated by a Lorentzian shape (appropriate to the resonance) at frequencies around $\tilde{\omega}$. In this region the initial distribution of the packet in the frequency space is small but still finite. The inset of figure 5(b) compares the decay rates ($\Gamma_L = \gamma/v_L$) of the reflected packets (the rear parts of the tails) calculated both analytically (equation (15)) and numerically. The coincidence of the slopes is excellent.

4.2. The Al–(Al/polymer)$_N$–H_2O system

For the system with a superlattice of nanometre periodicity considered in the previous subsection, the resonance frequency of the phonons is in the 100 GHz range. Experimental verification of the predicted results could be achieved by employing the picosecond-light-pulse method developed recently [1, 3, 14]. With this method, based on the pump-probe technique, the propagation of a high-frequency phonon pulse (longitudinal mode), with frequency in the 100 GHz range, has been studied for multilayered structures. If the layer thickness of the superlattice sandwiched in between the solid and liquid is increased up to the millimetre range, the resonance frequency is decreased down to several MHz, accessible to ultrasound transmission experiments [8]. Recently, an ultrasound imaging experiment on surface acoustic waves propagating on Al/polymer multilayers (the surface is parallel to the layer normal) was carried out with immersion transducers [9]. In this experiment the bilayer thickness is 1 mm and the frequencies of the ultrasound generated are 1 to 10 MHz. The extension of this experiment to the transmission experiment should be straightforward. The initial packet of rectangular shape considered is realized experimentally by the tone-burst excitation of ultrasound [8, 9].

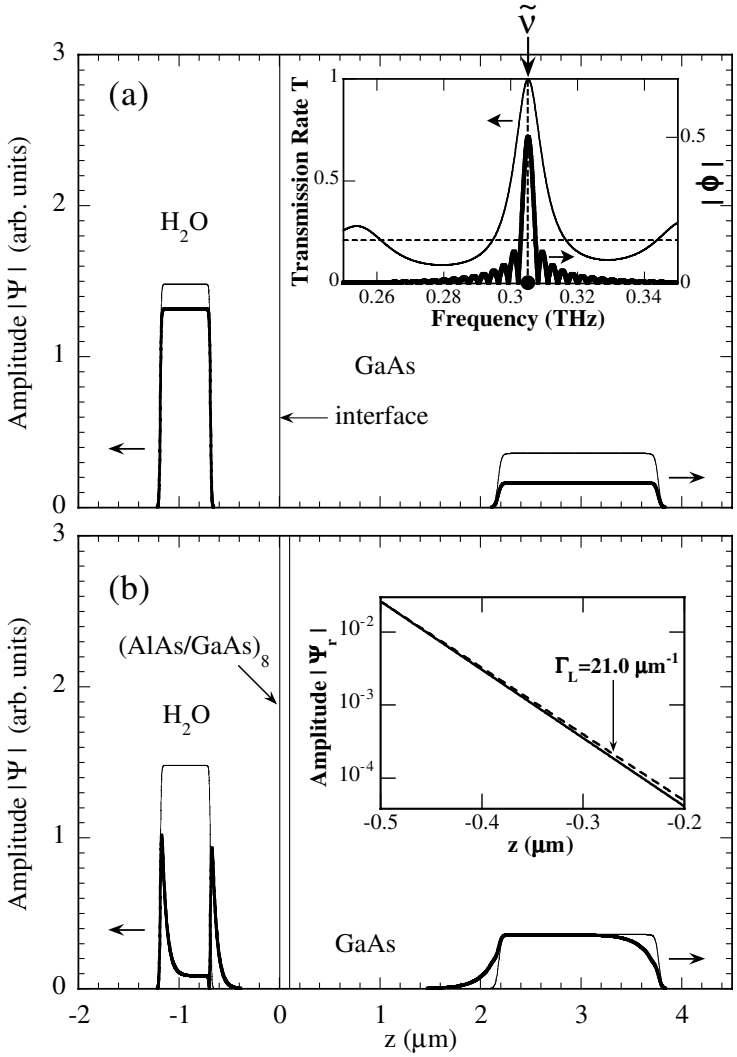

Figure 5. Shapes of the transmitted and reflected phonon packets (bold lines) at $t = 0.8$ ns after the wave front of the rectangular initial packet hits (a) a single GaAs/H_2O interface ($z = 0$) and (b) an AlAs/H_2O interface ($z = 0$) of the GaAs–(GaAs/AlAs)$_8$–H_2O structure. The initial packet propagates from the liquid side (the arrows indicate the direction of propagation of the transmitted and reflected packets). Thin lines show the positions at which the reference packets are expected to locate if they are perfectly transmitted through or reflected back from the interface. The inset of (a) illustrates the assumed frequency distribution of the initial phonon packet ϕ and the transmission rate near $\nu = \tilde{\nu} = 305$ GHz. The inset of (b) compares the decaying tails of the analytically (dashed line) and numerically calculated (solid line) reflected packets (the rear component).

Figures 6(a) and 6(b) compare the superlattice dispersion relation and the calculated transmission rate in the Al–(Al/polymer)$_N$–H_2O system with $N = 3$. We find a transmission peak at $\nu = \tilde{\nu} = 2.5$ MHz inside the lowest frequency gap of the phonons in the perfect, periodic Al/polymer superlattice. Unfortunately, the magnitude of the transmission peak is even smaller than that of the transmission rate ($T \approx 0.3$) for the single Al–polymer interface. (The peak height at $\tilde{\nu}$ becomes largest for $N = 3$, i.e., $N_{max} = 3$.) Thus the characteristic

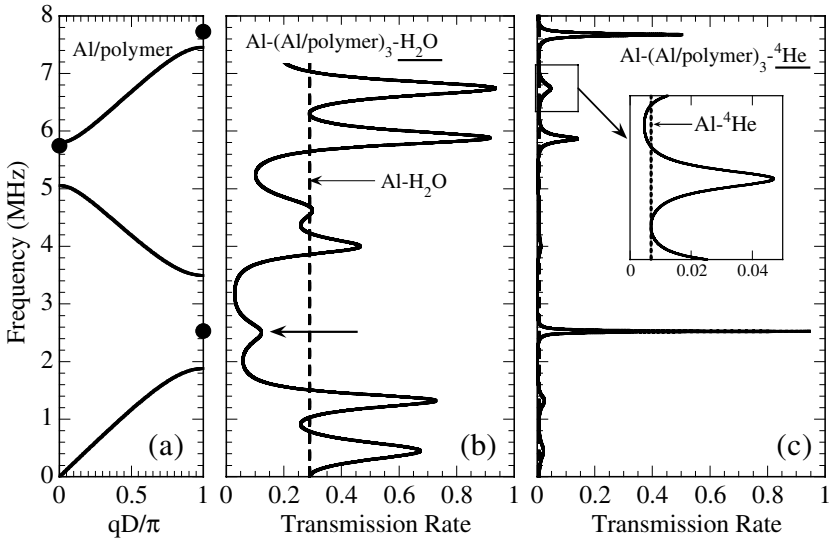

Figure 6. (a) Dispersion relations of the longitudinal sound in a perfect Al/polymer superlattice, (b) the transmission rate in an Al–(Al/polymer)$_3$–H_2O structure and (c) the transmission rate in the Al–(Al/polymer)$_3$–^{4}He structure. The thicknesses of the Al and polymer layers are 0.5 mm. The layer in contact with the liquid is a polymer (Crystalbond). Dots in (a) indicate the eigenfrequencies of the surface localized vibration in the semi-infinite Al/polymer superlattice and the dashed lines in (b) and (c) indicate the rates of transmission through the single Al–H_2O and single Al–^{4}He interfaces.

features of the transmitted and reflected packets discussed in section 4 should not be observed even if an ultrasound packet with peak amplitude at $\tilde{\nu} = 2.5$ MHz is excited. If water is replaced with liquid helium ($Z_{^4\mathrm{He}}/Z_{\mathrm{H_2O}} = 0.02$) the enhanced transmission at $\nu = \tilde{\nu}$ becomes almost perfect ($T \simeq 1$) for $N = 3$ (figure 6(c)). However, the experiment at liquid-helium temperatures would not be practical for a sample incorporating a polymer.

In figure 6(b) there exist a couple of transmission peaks with $T \simeq 0.9$ inside the frequency band. These enhancements of the transmission are not due to the resonance with surface localized vibrations but rather arise from the resonance with extended vibrational states in the multilayered structure considered. The number of transmission peaks in a frequency band coincides with the number of bilayers N in the structure†. Qualitatively, this effect is analogous to the resonant tunnelling of a particle through discrete energy levels of multiple quantum wells. We note that an energy level in a potential well is split into N levels if N potential wells are coupled together. This number N of split energy levels corresponds to the number of peaks in the ultrasound transmission in a frequency band and the locations of the peaks define another kind of resonance frequency ν_0.

If the stacking order of the constituent layers in the Al/polymer multilayers is interchanged, i.e., an Al layer (B layer) is adjacent to water, we find a peak in transmission with $T \simeq 1$ at $\nu \sim 6$ MHz. This is shown in the inset of figure 7. The calculated transmitted and reflected packets for an incident rectangular packet (width $2a = 2$ cm) with peak frequency $\nu = \nu_0 = 6.04$ MHz have been plotted in figure 7. The transmitted and reflected packets take essentially the same characteristic shapes as in figure 5 for the case of resonance with the vibrations localized at the superlattice–liquid interface.

† This number N is effectively 2 for figure 6 because S = A = Al, but it is 3 for figure 7 below because S = Al and B = polymer.

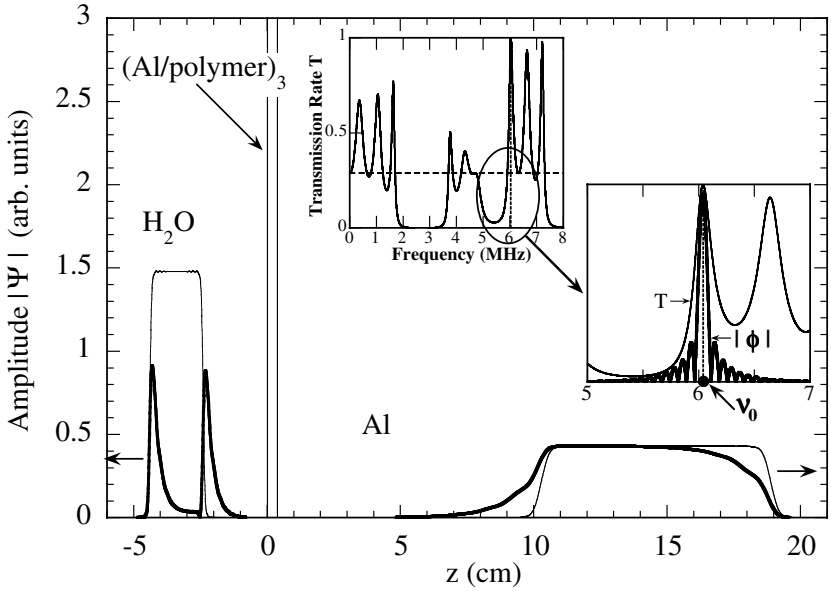

Figure 7. Shapes of the transmitted and reflected phonon packets (bold lines) at a time $t = 50\ \mu$s after the wave front of the rectangular initial packet hits the interface ($z = 0$) between H_2O and Al/polymer multilayers in the Al–(polymer/Al)$_3$–H_2O structure. The initial packet propagates from the H_2O side (the arrows indicate the direction of propagation for the transmitted and reflected packets). Thin lines show the positions at which the reference packets are expected to situate if they are perfectly transmitted through or reflected back from the interface. The inset shows the transmission rate of the longitudinal sound wave in the structure considered (the layer in contact with water is aluminium). The assumed frequency distribution ϕ of the initial packet is also shown.

5. Concluding remarks

The phonon transmission through an interface between a solid and a liquid can be enhanced anomalously by putting a periodic multilayered structure, or a superlattice, at the interface. We have shown that this enhancement is really dramatic in the GaAs–(GaAs/AlAs)$_N$–H_2O system at a frequency $\tilde{\nu}$ inside a frequency gap of the perfect GaAs/AlAs superlattice. Then we studied for the same structure characteristic features associated with the phonon-packet propagation in the $\nu \simeq \tilde{\nu}$ region. For the Al–(Al/polymer)$_N$–H_2O system employed recently in ultrasound transmission experiments [9] a similar enhancement in transmission in a frequency gap is also seen, but it is very small. The effect can be enhanced considerably if the liquid is changed to ^{4}He (from H_2O) but the experiment with liquid ^{4}He is intractable at room temperatures. However, for the Al–(Al/polymer)$_N$–H_2O system the transmission peaks with $T \simeq 1$ can be seen at an isolated frequency ν_0 inside the frequency band of the perfect Al/polymer superlattice. In both cases the magnitude of the transmission peak is sensitive to the number of bilayers inserted.

We have studied for the above two systems the time evolution of the transmitted and reflected phonon packets for an initial packet of rectangular shape. Several interesting aspects are predicted for the transmitted and reflected packets in asymptotic regions far away from the solid–liquid interface. In particular, if the transmission peak in the multilayers (near $\tilde{\nu}$ or ν_0) is well approximated by a Breit–Wigner form appropriate to the resonance, the reflected packet adopts a double-peak structure with exponentially decaying tails. The transmitted packet also has a tail produced by the decay of the resonance state. Thus we conclude that the double-peak

structure of the reflected packet is universal if an incident rectangular packet interacts with a resonant state in a periodic, multilayered structure where the phonon packet propagates. These new simulated results for elastic, periodic, multilayered structures should be confirmed experimentally using a picosecond-light-pulse method or an ultrasound imaging technique in the reflection geometry.

Acknowledgment

This work was supported in part by a Grant-in-Aid for Scientific Research from the Ministry of Education, Science and Culture of Japan (Grant Number 09640385).

References

[1] For recent experimental measurements, see
Tas G and Maris H J 1997 *Phys. Rev.* B **55** 1852
[2] Kato H 1999 *Phys. Rev.* B **59** 11 136
[3] Chen W, Lu Y, Maris H J and Xiao G 1994 *Phys. Rev.* B **50** 14 506
[4] Mizuno S and Tamura S 1996 *Phys. Rev.* B **53** 4549
[5] For localized vibrations at a substrate–superlattice interface, see
Camley R E, Djafari-Rouhani B, Dobrzynski L and Maradudin A A 1983 *Phys. Rev.* B **27** 1427
Bria D, El Boudouti E H, Nougaoui A, Djafari-Rouhani B and Velasco V R 1999 *Phys. Rev.* B **60** 2505
[6] Mizuno S 2001 *Phys. Rev.* B at press
[7] Mizuno S and Tamura S 1994 *Phys. Rev.* B **50** 7708
[8] Weaver R L, Hauser M and Wolfe J P 1993 *Z. Phys.* B **90** 27
[9] Vines R E, Wolfe J P and Every A G 1999 *Phys. Rev.* B **60** 11 871
[10] For the calculation of the phonon transmission rate in a superlattice, see
Mizuno S and Tamura S 1992 *Phys. Rev.* B **45** 734
[11] Wigner E P 1955 *Phys. Rev.* **98** 145
[12] Hauge E H and Støvneng J A 1989 *Rev. Mod. Phys.* **61** 917
[13] Landauer R and Martin Th 1994 *Rev. Mod. Phys.* **66** 217
[14] Perrin B, Bonello B, Jeannet J-C and Romatet E 1996 *Physica* B **219+220** 681